Bulletin of the JSME Vol.9, No.5, 2015
Journal of Advanced Mechanical Design, Systems, and Manufacturing

Bending strength simulation of asymmetric involute tooth gears

Tomoya MASUYAMA*, Yasunari MIMURA* and Katsumi INOUE**
*National Institute of Technology, Tsuruoka College
104 Sawada, Ino-oka, Tsuruoka 997-8511, Japan
E-mail: masu@tsuruoka-nct.ac.jp
**Professor Emeritus of Tohoku University
6-6 Aoba Aramaki, Aoba-ku, Sendai 980-8579, Japan

Received 4 September 2015

Abstract
Aiming at high load capacity, the design of the tooth profile which is not caught by the conventional profile is performed. Root stresses are calculated by 2D-FEM for various profile gears: 1) completely bilateral symmetry, 2) symmetry pressure angle and asymmetry fillet curve, and 3) asymmetry tooth. Reduction of root stress is brought by adoption of a higher pressure angle, and larger curvature radius of the fillet. Root stress of 40degrees of pressure angle tooth due to the unit tip load is reduced of 30% rather than ISO standard tooth. Nevertheless, the torque capacity for bending strength of higher pressure angle gears will not increase because of small base radius and low contact ratio. Tooth profile which has 25degrees of pressure angle with larger tooth root radius expect to perform higher torque capacity. The fatigue strength simulation method is also applied to those gears. The strength of tooth is estimated by comparing the local stress and the local strength restricted by defect size. Since the dangerous volume which takes higher stress becomes narrow, the profile with small width of tooth space expects that strength will enhance. According to the simulation, higher load capacities are expected in high pressure angle teeth than FEM calculation.

Key words : Gear, Strength, Tooth profile, Simulation, Asymmetry tooth, Pressure angle

1. Introduction

In order to enhance the load capacity of gears, researchers take notice in the asymmetric tooth gears. Asymmetric gear which has higher pressure angle of back tooth aiming to improve banding strength has been analyzed (Deng, et al., 2003). Brown et al. (Brown, et al., 2010) investigate the asymmetric tooth from both point of view of bending and scuffing. Kruger et al. (Kruger et al., 2013) analysed root stress of asymmetric gear by the boundary element method. Recently in Japan Society of Mechanical Engineers, improvement of contact strength by higher pressure angle is paid attention (Morikawa, 2013). However, they have not mentioned to torque capacity for bending considering the single tooth contact. This paper attempts the design of a tooth profile that has a higher load capacity. The root stress by change of pressure angle is analysed by FEM. Furthermore, the bending fatigue strength of tooth paying attention to the torque capacity is investigated by a simulation method based on inclusion distribution (Masuyama, et al., 2013).

2. Fundamental considerations on the change of tooth profile

A change in tooth profile is considered to be a factor that has an influence on torque capacity. Figure 1 shows the contact condition of gear teeth. The subject tooth shown in purple is in a condition of highest point of single tooth contact (HPSTC). According to the figure, factors 1-6 and can be considered.

(1) The tooth thickness of the root section

The square of the tooth thickness operates as a section modulus against tooth bending

Paper No.15-00485
[DOI: 10.1299/jamdsm.2015jamdsm0071]

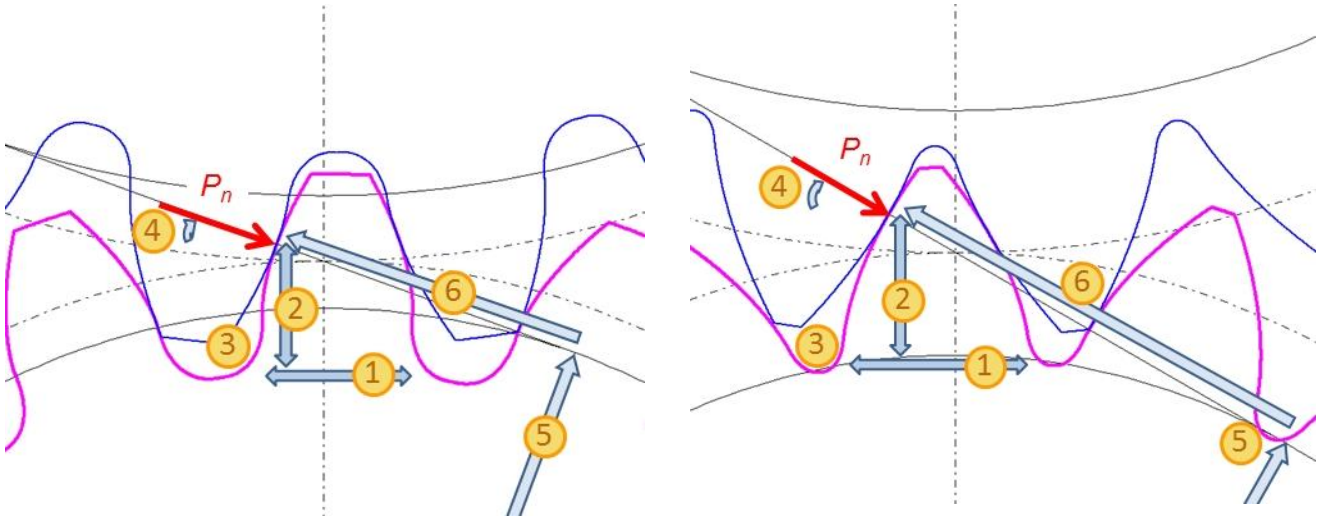

Fig. 1 Factors that affect torque capacity (left: low pressure angle, right: high pressure angel).

(2) The distance from the root of the tooth to the load position
This determines the bending moment
(3) Stress concentration according to the tooth fillet curve
(4) Pressure angle
This can be separated into a component force that influences the bending of the tooth and a component force that compresses the tooth in the direction of the tooth root.
(5) Base radius r_b
The relationship between torque T and the normal load to the tooth P_n is $T = P_n \times r_b$.
(6) Radius of curvature of tooth profile
The curvature effects on the on the contact pressure.
The above have an effect on torque capacity.

3. FEM model

3.1 Rack tool design and tooth profile creation

First, the form of the rack tool was designed to be a parametric and the tooth profile was created by rolling the pitch line of the rack on the pitch circle of the gear blank. In order to simplify to understand, the following restrictions were established.

I. The factors that are modified in the parametric are pressure angle α_1 on the right cutter face, pressure angle α_2 on the left,
II. right cutter tip corner radius r_{f1}, and left cutter tip corner radius r_{f2}. r_{f1} and r_{f2} are normalized by the module m. r_{f1} and r_{f2} are changed in steps of 0.01.
III. The cutter tip corner is tangent to a straight line and does not have an angle.
IV. The dedendum on the rack, that is, the addendum of the gear, is $1 \times m$.
V. The addendum of the rack is maintained at $1.25 \times m$.
VI. The cutter tip corner radius is of a range such that gears do not statically interfere with meshing gears.
VII. The addendum modification coefficient when generating the gears is 0.

Figure 2 shows an example of the rack profile. Marks of I to V in the figure are corresponds to items above. In this paper, the rack and the tooth are expressed by the code α_1-α_2-r_{f1}-r_{f2}. For example, the case of α_1=35degrees, α_2=20degrees, r_{f1}/m=0.25, and r_{f2}/m=0.15 is expressed as 35-20-25-15 on Fig. 3. If the pressure angle of a right tooth face as shown in this example is made large, the tool tip moves to the transverse position as depicted on Fig. 3.

Here, concerning the item VI, The r_f requires to be $0.25/(1-\sin\alpha)$ in order to keep addendum height $1 \times m$ of straight line of cutter edge under the condition of item V. The gear which processed by the cutter with larger tip corner than threshold r_f interfere at root when mesh with rack. Nevertheless, the starting point of meshing moves to tip side according as number of tooth reduces. Interference under statical profiles of conjugate gears of z_1=18 and z_2=25 does

[DOI: 10.1299/jamdsm.2015jamdsm0071]

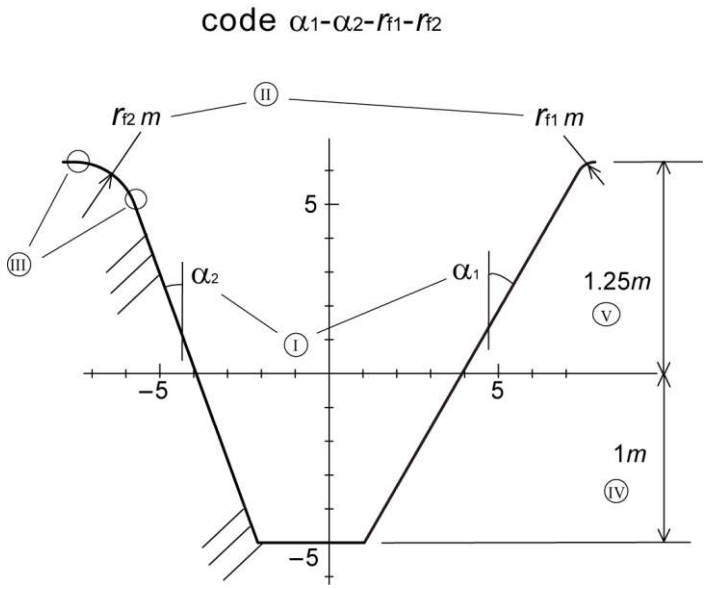

Fig. 2 Parameters expressing the rack form.

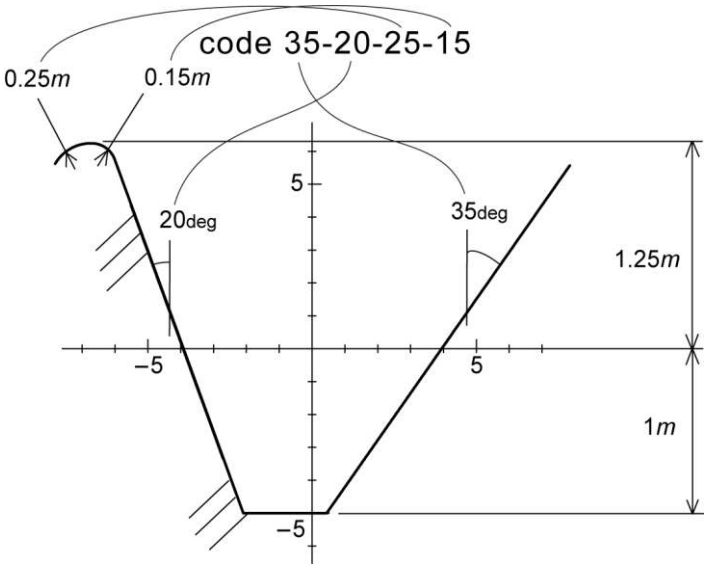

Fig. 3 An example of a rack form.

not occur when using tooth profiles referring in this paper. It was confirmed by coordinate data of tooth profiles.

Examples of a tooth profile created are shown in Fig. 4. The ISO standard tooth profile is described by the black narrow line.

3.2 FEM mesh

Point data for the tooth profiles created in Fig. 4 were sampled at an appropriate interval and made nodes on the outline. The node interval at the root section is approximately 0.15 mm. To reduce the number of elements and nodes, an objective tooth and adjacent teeth were created and the rest of the gear was made a cylindrical form. The inner nodes were generated automatically by the Delaunay method (Taniguchi, 1992). The number of elements and the number of nodes differ slightly according to the model, but in the case of 30-20-44-01 there are 4492 elements and 4726 nodes. An example of the mesh is shown in Fig. 5.

[DOI: 10.1299/jamdsm.2015jamdsm0071]

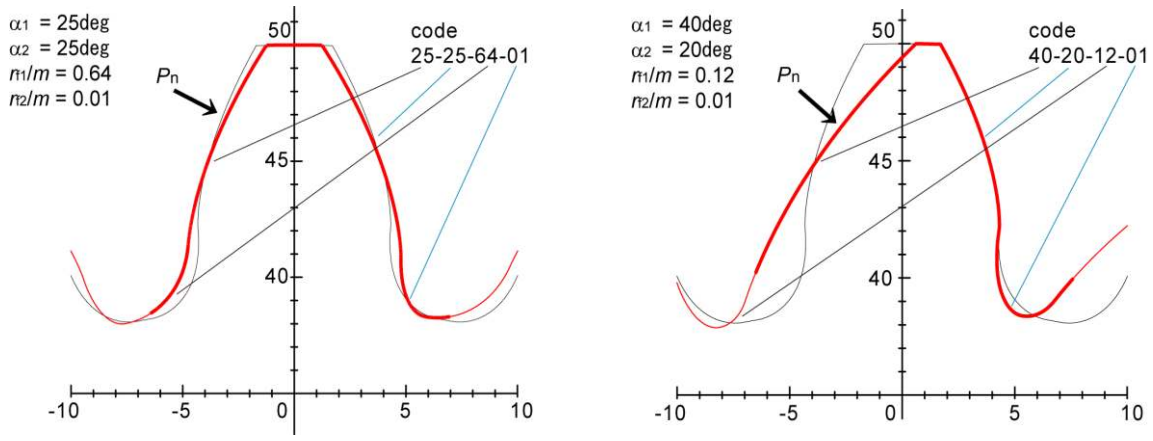

Fig. 4 Examples of created tooth profiles.

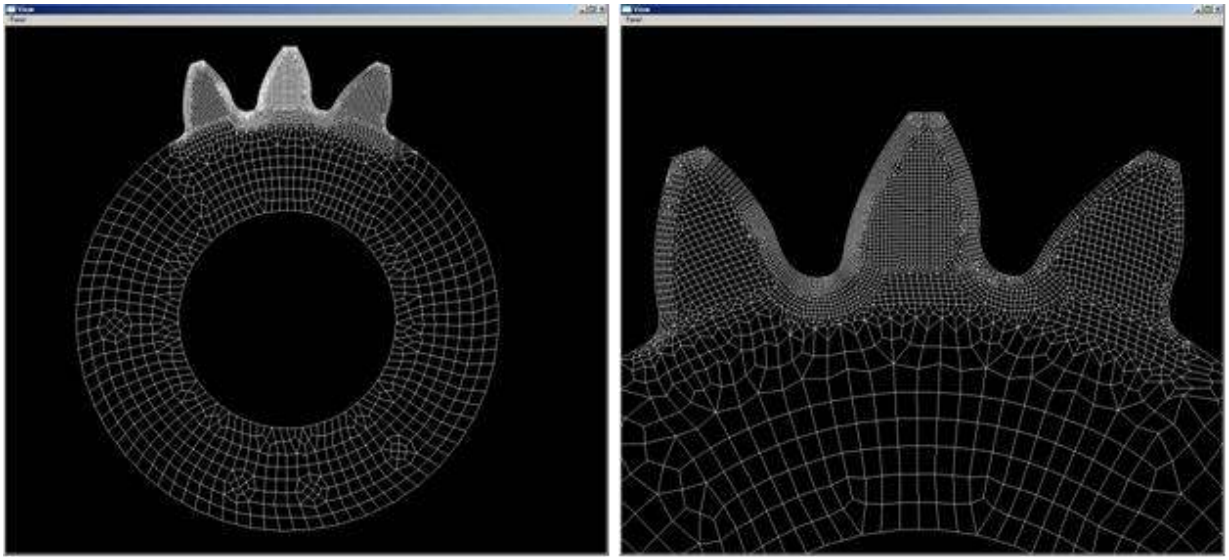

Fig. 5 Example of FEM model.

4. Stress analysis

4.1 Effect of the cutter tip corner

Figure 6 shows the maximum root stress when the pressure angle on both the left and right tooth surfaces is made 20degrees and a unit load is applied 0.5mm from the tip with respect to a tooth for which the cutter tip corner radius is changed. If r_{f2} is increased while maintaining r_{f1}=0.38, it is possible to increase to 0.56. Thereupon, stress becomes as much as 3% smaller in comparison to the ISO standard 20-20-38-38. The root form on the loading side does not change and so presumably bending stress is reduced by the thickness increasing. Values of r_{f1}= r_{f2}=0.47; code 20-20-47-47, fulfilled conditions V and VI shown in section 3 with the left and right cutter tip being equal. Analysis was carried out on 20-20-56-38, which is a form given by reversing 20-20-38-56 on the horizontal. It can be said that the stress being low in comparison to 20-20-38-56 is caused by the relief of stress concentration due to the radius of curvature of the root becoming large. Also, setting z_2=25 for the meshing gear meant that $r_{f1} \leqq 0.65$ satisfied condition VI. As can be seen from the diagram, if the tooth thickness is made as large as possible and the cutter tip corner on the loading side is made large, the maximum root stress becomes smaller. Accordingly, only tooth profiles that satisfy conditions V and VI and that result in a maximum r_{f1} are used in the following analysis.

[DOI: 10.1299/jamdsm.2015jamdsm0071]

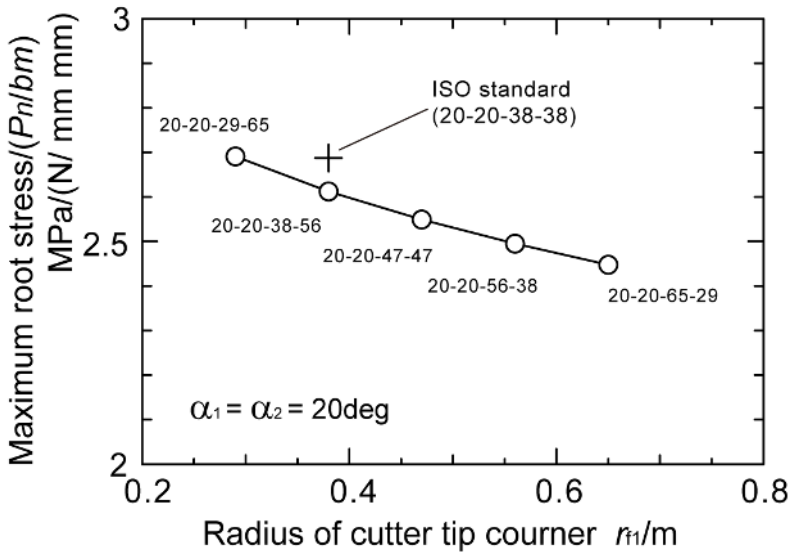

Fig. 6 Effect the tool nose radius on the maximum root stress.

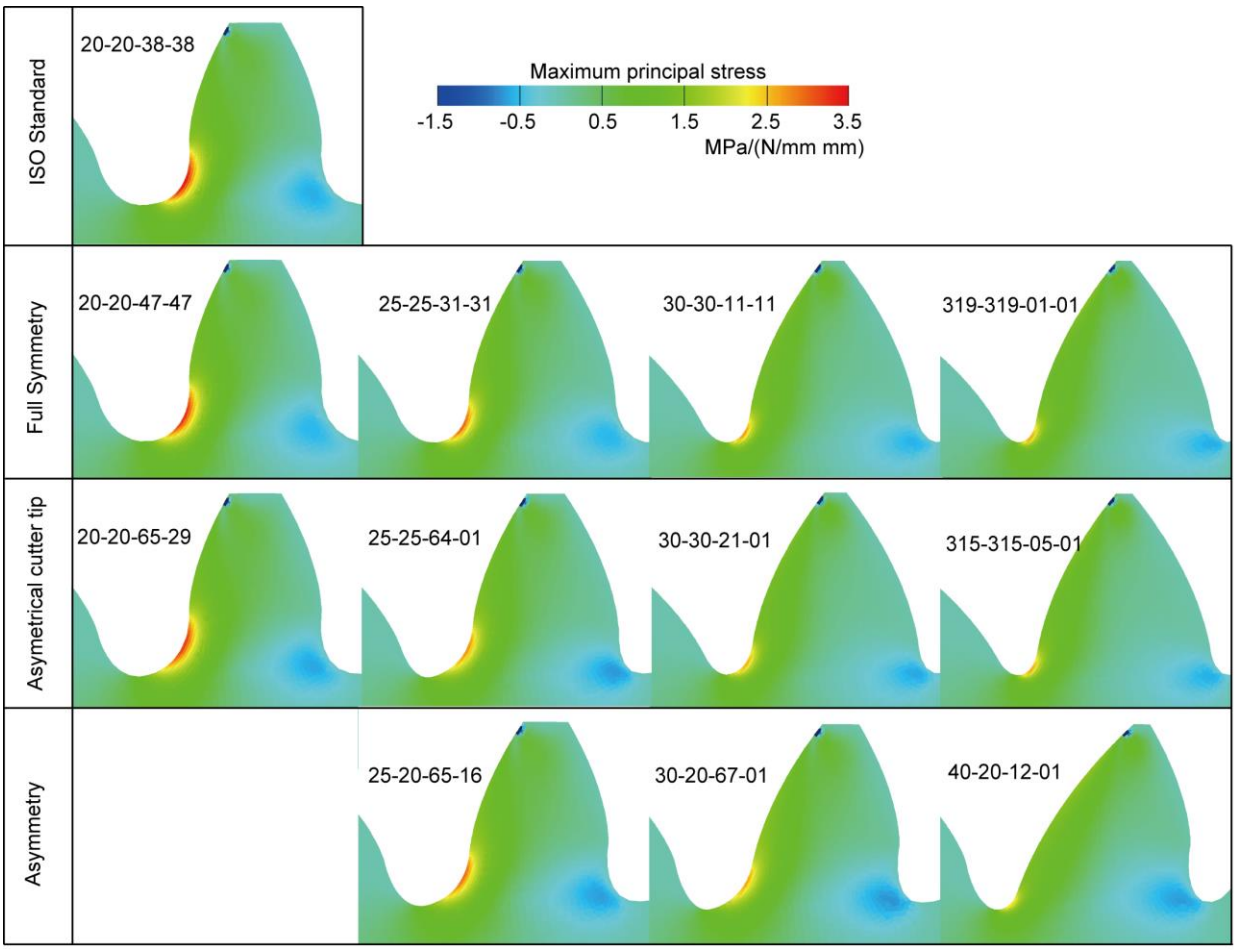

Fig. 7 Distribution of maximum principal stress when load applied to tip.

[DOI: 10.1299/jamdsm.2015jamdsm0071]

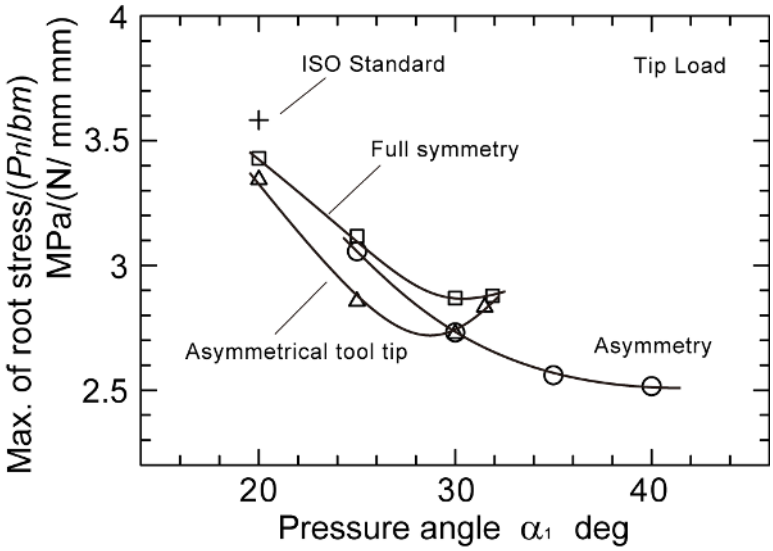

Fig. 8 Maximum root stress when load applied to tip.

4.2 Analysis of stress by tip load

Contour diagrams of maximum principal stress due to tip load are shown in Fig. 7. Also, the maximum values of the principal stress are plotted in Fig. 8. The leftmost column of Fig. 7 is for the case of pressure angle of 20degrees for both the left and right tooth surfaces. The uppermost line is the ISO standard 20-20-38-38; the second line is for 20-20-47-47, which has full symmetry and for which the tip corner can be made the largest; and the third line is for 20-20-65-29, for which the tip corner on the contact side is made a maximum. Next, we compare the second level. On this level, on which the tooth profiles with full symmetry teeth are arranged, it can be seen that the tooth thickness at root increases as the pressure angle increases and the bending stress decreases. In the comparison in Fig. 8, the maximum stress increases slightly for 315-315-01-01 in comparison to 30-30-11-11. This is presumably because the spacing between adjacent teeth decreased, radius of curvature decreased and stress concentration increased. Finally, the fourth level arranges the results for asymmetrical teeth. The pressure angle for the right tooth was 20degrees. At a pressure angle of 25degrees on the contact side, the tooth thickness decreases in comparison to a symmetrical tooth and bending stress increases. The maximum stress in 30-30-21-01 and 30-20-67-01 of a pressure angle of 30degrees was almost equivalent. This is presumably because the size of the tooth thickness works effectively in the former and the fillet stress concentration mitigation is effective in the latter. If the contact side pressure angle is greater than this, an asymmetrical tooth profile by which the width or curve radius of the tooth spacing can be increased is effective in decreasing stress.

4.3 Analysis of stress with load on the highest point of single tooth contact

When investigating the bending load capacity of a tooth, the condition of the highest point of single tooth contact (HPSTC) should be considered. As was shown in Fig. 1, if the pressure angle is increased, the HPSTC migrates to the tip and the bending moment is large. Accordingly, the HPSTC is calculated with the tooth subject to analysis as z_1=18 and the meshing gear as z_2=25, and the stress was analysed by HPSTC load. The maximum value of the principal stress for each tooth is plotted in Fig. 9. It can be seen that, in comparison to Fig. 8, the stress increases in the region where the pressure angle is large. In evaluating the performance of a gear, it is best to make a comparison by torque transmission capacity. When an equivalent torque is delivered, the normal load increases with pressure angle. The tooth root stresses when the HPSTC load which brings torque of 1Nm is applied are plotted in Fig. 10. A remarkable rise in bending stress can be seen in the region where pressure angle is large. Stress decreased at high pressure angles in Fig. 8. However, focusing on the meshing conditions and the transmission torque, the range of pressure angle of 25-28degrees was found to have an excellent torque capacity for bending.

[DOI: 10.1299/jamdsm.2015jamdsm0071]

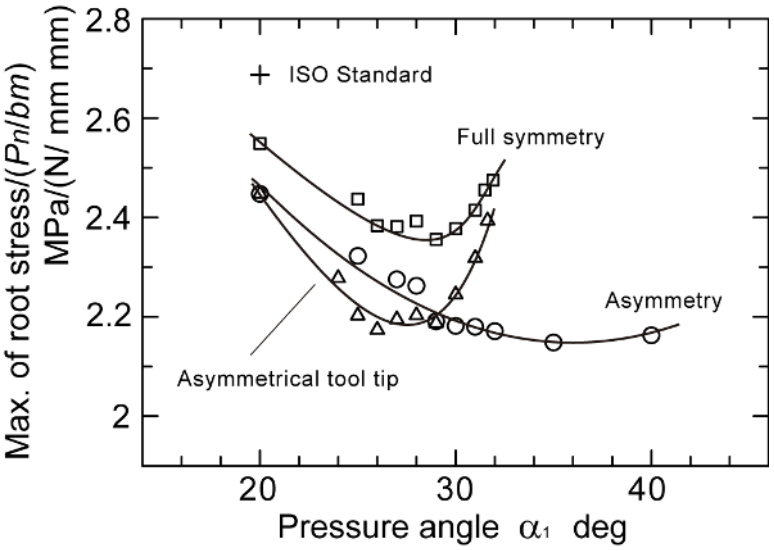

Fig. 9 Maximum root stress caused by HPSTC loading.

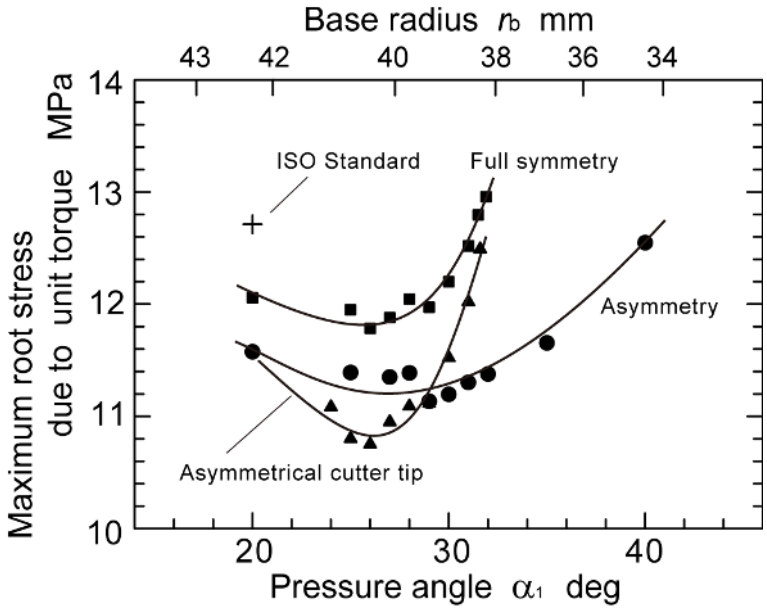

Fig. 10 Maximum root stress due to unit torque.

5. Bending strength simulation

5.1 Strength computation with identifying principal defect

The authors have proposed a simulation method (Masuyama and Inoue, 2002a) which estimate the bending fatigue strength of gear tooth taking defect size and as a parameter. In the first step, defects of various sizes are distributed in an imaginary material. The maximum principal stress σ_i at the position of defect i is calculated by FEM in the second step. In the next step, the material's own strength, σ_i *, is evaluated by substituting the defect size and other required values into formula (1) (Masuyama et al., 2002b). Here, H is Vickers hardness and A_i (μm)^2 is the projected area of defect.

$$\sigma_i^* = 0.98\frac{(H+120)}{\left(\sqrt{A_i}\right)^{1/6}}\left[\frac{1}{2}\right]^{\alpha} \qquad (1)$$

$$\alpha = 0.226 + H_V \times 10^{-4}$$

[DOI: 10.1299/jamdsm.2015jamdsm0071]

Then, stress σ_i is compared with strength σ_i * at every position of defect. σ_i is smaller than σ_i * at first, since the initially applied load is low. The load is increased step-by-step until stress σ_i at a certain defect, which maximizes the ratio of bending stress to material's strength, equals strength σ_i. The load at this stage is represented by the maximum stress at the fillet and indicates the strength of the gear tooth which breaks at the defect position. This defect evidently defines the limit of gear strength; therefore, it is called the principal defect.

The position of inclusions in the imaginary material is placed randomly. Sizes of inclusions are applied to the Weibull distribution function. In simulations, we determine the size of inclusions by generating random numbers that follow the distribution function.

$$F(t) = 1 - \exp\left\{-\left(\frac{t-\gamma}{\eta}\right)^m\right\}$$

Here, $F(t)$ is the cumulative frequency function of t, and t indicates the square root of inclusion area $\sqrt{A_i}$. Parameters obtained by observation of JIS SCM420 steel are shown in Table 1. The density of inclusions is 52 pieces/mm^2. The accuracy of this computation method has been confirmed by comparing with fatigue test results as shown in Fig. 11. The mean strength obtained by the simulation is 8% higher than the experimental result and the standard deviation is 33% smaller than it. Bewaring with it shows dangerous side for the strength design, the simulation method is adopted in this paper. When comparing between simulation results, those differences are ignore.

Table 1 Weibull parameters of inclusions for simulation.

	$A_i < A_{i\ th}$	$A_{i\ th} < A_i$
$A_{i\ th}$	17	
γ	1.000	1.000
η	1.475	0.187
m	1.353	0.356

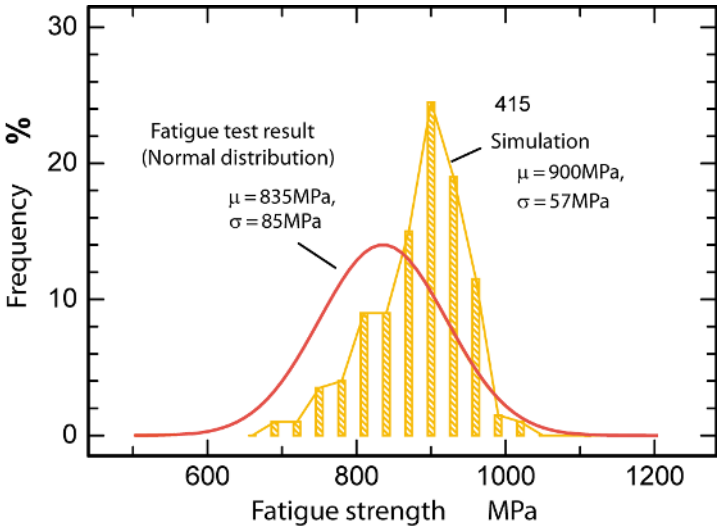

Fig. 11 Distribution of computed fatigue strength.

[DOI: 10.1299/jamdsm.2015jamdsm0071]

5.2 Investigation of bending strength

The results of the simulation with load on the HPSTC are shown below. Tooth hardness is made uniform at 700Hv and residual stress is not taken into consideration. 200 strength estimations were made for each tooth profile and the distribution of strength was found. The simulation results are expressed by maximum root stress and the average values

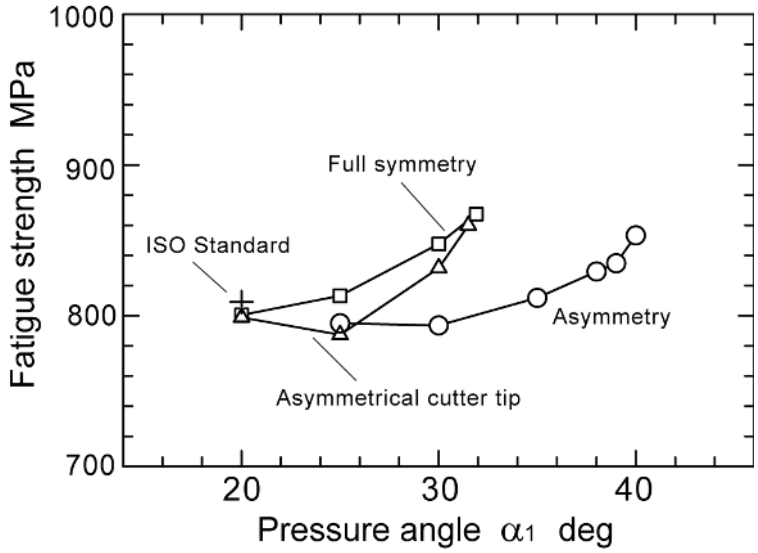

Fig. 12 Results of the bending strength simulation (average values for trials on 200 teeth).

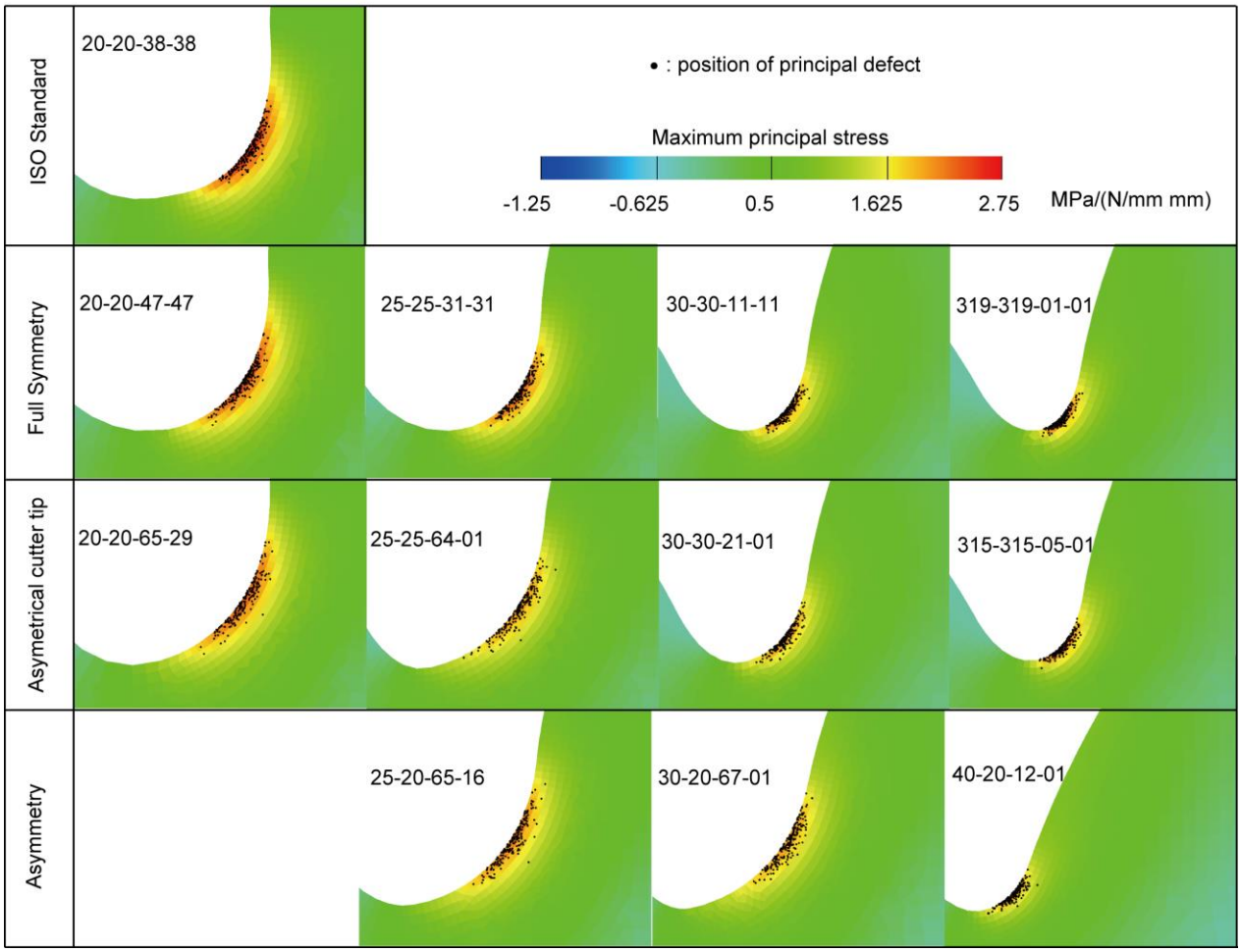

Fig. 13 Distributions of principal defect locations and that formed fracture origins and stress.

[DOI: 10.1299/jamdsm.2015jamdsm0071]

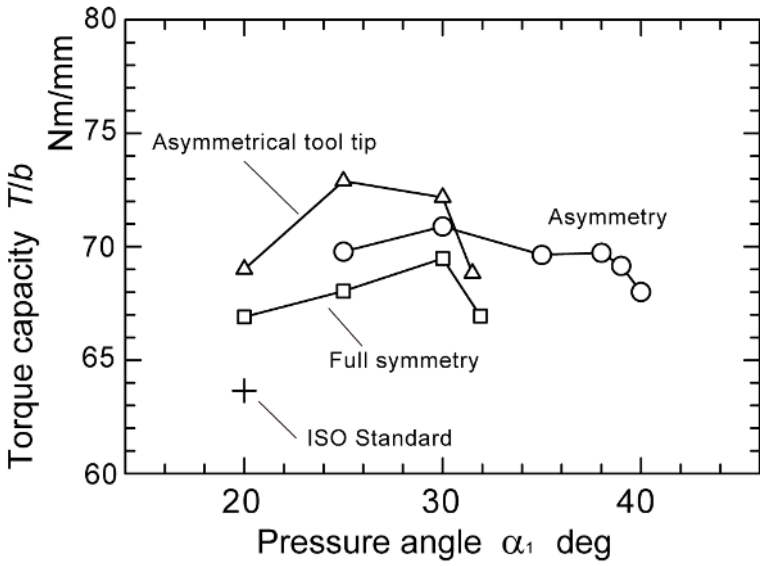

Fig. 14 Strength simulation results (comparison by torque capacity).

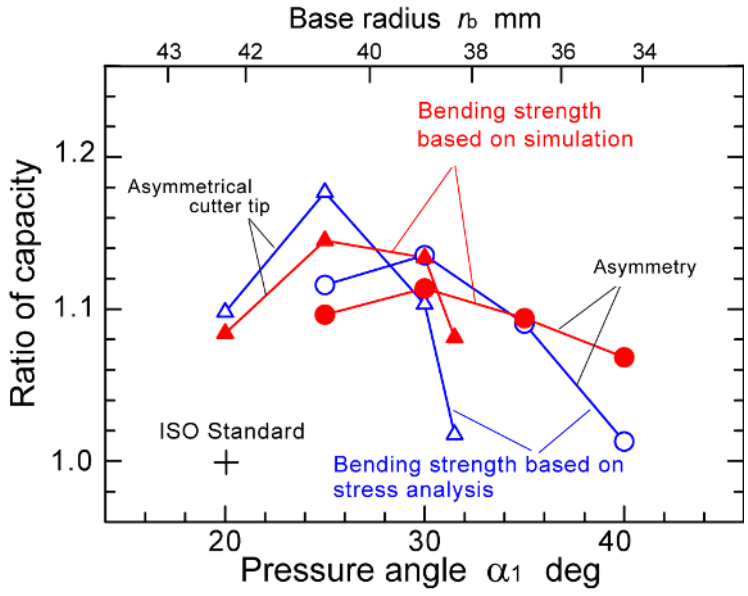

Fig. 15 Difference in load capacity due to change in tooth profile.

of the strength distributions are plotted in Fig. 12. In every case, strength increased with pressure angle. Also, the result was that the strength of the full symmetrical tooth was high. This can be explained from the perspective of dangerous volume. That is, even if the maximum stress in a tooth component is equivalent, as the region exposed to a high stress becomes small, the probability that an inclusion is contained in that area lowers, statistically resulting in a high strength accordingly. Figure 13 is the result of drawing the stress distribution of each tooth and the locations of the principal defect that is the fracture origin. It is found that the region of high stress is narrow and the locations of the fracture origins are distributed in a narrow range for right side in the figure, which exhibited a high strength in Fig. 12. Re-calculating the results of Fig. 12 as transmission torque gives Fig. 14. From the simulation, the endurance tooth normal load P_s which gives fatigue strength is calculated by using the relationship shown in Fig. 13. Then transmitted torque T_c by load P_s, which matches for the capacity of tooth, is obtained and shown in Fig. 14. The torque capacity is low for tooth profiles for which the bending stress becomes large with respect to the same normal load. Teeth with a high pressure angle are also unfavorable for torque transmission.

[DOI: 10.1299/jamdsm.2015jamdsm0071]

5.3 Summarize of strength simulation

We will now summarize in Fig. 15 differences in tooth torque capacities according to the change of tooth profile investigated above. In order to avoid complicating the graph, the full symmetrical teeth are excluded. The diagram expresses the results in terms of a ratio of torque capacity with respect to 20-20-38-38, that is, an ISO standard tooth. For a start, the maximum root stresses are compared by blue lines with blue marks in Fig. 15. Triangles indicate a tooth for which the pressure angle is symmetrical and for which the cutter tip corner differs, and circles indicate asymmetrical tooth. This line is drawn by ratio of calculation results shown in Fig. 10. Next, red lines with red marks express the torque capacity computed by the simulation. According to the red lines, higher load capacities are expected in high pressure angle teeth than FEM calculation, in either case the left and right pressure angle is made 25degrees and the tooth root curve on the load side is made large (25-25-64-01) shows the best capacity.

6. Conclusions

The torque capacities of tooth profiles that were made bilaterally asymmetric with the aim of further increasing load capacity were investigated by a simulation method based on stress analysis and inclusion distributions. The main results were as follows:

1. Bending stress can be reduced by increasing the tooth thickness of the root section through changing the pressure angle or adjusting the root fillet curve. Increasing the radius of curvature of the root fillet curve and decreasing the stress concentration is effective.
2. Considering the relationship between the location of the highest point of single tooth contact, the normal load, and the transmission torque, increasing the pressure angle does not contribute significantly to an increase in load capacity with respect to bending.
3. The left and right pressure angles are made 25degrees and the tooth root curve on the load side is made large (25-25-64-01) shows the best capacity according to either stress analysis or strength simulation.
4. Higher strength is expected from the simulation method in high pressure angle tooth which has larger than 30degrees, from a view point of the reduction of dangerous volume.
5. Although torque capacity for bending decreases when using higher (>35degrees) pressure angle, it is effective for reduction of contact pressure caused by larger curvature radius of tooth.

References

DENG, G., NAKANISHI, T. and INOUE, K., Bending Load Capacity Enhancement Using an Asymmetric Tooth Profile, JSME International Journal, Series C, Vol.46, No.3, (2003), pp.1171-1177.

D. Kruger, I. Romhild, H. Linke, J. Brechling and R. Hess, Increasing the Load Capacity of Gear Teeth by Asymmetric Gear Tooth Design, International Conference on Gears 2013, VDI-Berichte Nr. 2199, (2013), pp. 1327-1340.

F. W. Brown, S. R. Davidson, D.B. Hanes, D.J. Weires and A. Kapelevich, Analysis and Testing of Gears with Asymmetric Involute Tooth Form and Optimized Fillet Form for Potential Application in Helicopter Main Drives", AGMA Technical Resources, 10FTM14(2010).

Masuyama, T. and Inoue, K., Computation of Fatigue Strength of Carburized Gears Based on Simulated Distribution of Defects, International Conference on Gears, VDI-Berichte Nr. 1665, (2002), pp.421-434.

Masuyama, T., Kato, M., Inoue, K. and Yamashita, T., Evaluation of Bending Strength of Carburized Gears Based on a Quantification of Defect Size in the Surface Layer, Transactions of the ASME, Journal of Mechanical Design, 124-3, (2002), pp.533-538.

Masuyama, T., Mimura, Y. and Inoue, K. Strength simulation of asymmetric involute tooth gears, International Conference on Gears 2013, VDI-Berichte Nr. 2199, (2013), pp. 1367-1378.

Morikawa, K., Improvement of strength by change of tooth parameters, Report of the Research Committee 251, The Japan Society of Mechanical Engineers, (2013), pp.75-85. (in Japanese)

Taniguchi, T., Automatically Meshing for Finite Element Method, Morikita Publishing Co., Ltd., (1992), (in Japanese)

[DOI: 10.1299/jamdsm.2015jamdsm0071]